QUARKS: Brazilian Electronic Journal of Physics, Chemistry and Material Science
journal homepage:
https://periodicos.ufjf.br/index.php/quarks
e-ISSN: 2674-9688

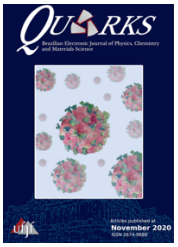

A new matrix of MALDI-TOF MS derivative of 9-aminoacridine for lipid identification in positive ions mode

Jefferson S. Martins[a,b], Fabio Zappa[a], Adilson David da Silva[c], Roberto R. Pinho[a], Thiago P. Silva[d], Kátia B. Amaral[d], Rosana Gentile[e], Rossana C. N. Melo[d], Welber G. Quirino[a], Pedro Henrique F. Stroppa[c]

[a]*Departamento de Física, Federal University of Juiz de Fora, Minas Gerais, 36036-900, Brazil.*

[b]*UNESA Productivity Research Program Scholarship, Universidade Estácio de Sá (UNESA), Juiz de Fora, Minas Gerais, 36030-142, Brazil.*

[c]*Departamento de Química, Federal University of Juiz de Fora, Minas Gerais, 36036-900, Brazil.*

[d]*Laboratory of Cellular Biology, Department of Biology, Federal University of Juiz de Fora, Minas Gerais, 36036-900, Brazil.*

[e]*Laboratory of Biology and Parasitology of Wild Reservoir Mammals, Oswaldo Cruz Foundation, Rio de Janeiro, RJ, Brazil.*

Article history: Received: August 2020; Revised: September 2020; Accepted: October 2020. Available online: November 2020.
https://doi.org/10.34019/2674-9688.2020.v3.30757

Abstract

Matrix-assisted laser desorption/ionization (MALDI) has evolved to become a well- established technique during the last decades. Because of matrix peak interference in the low molecular-weight region, however, new matrices are often studied with the purpose of improving the spectral quality under m/z 500. Herein, we present the substance 2,4,5,7-tetranitro-9-aminoacridine (TNA) as a suitable alternative matrix for lipid detection in the positive-ion mode. TNA is obtained from 9-aminoacridine, a matrix commonly used to analyze lipids in negative-ion mode, with the addition of 4 nitro groups through a synthetic path. The procedure results in a highly conjugated system that presents a bigger electronic dispersion and therefore higher UV absorption. First, we demonstrated the high sensitivity of TNA for retinol. Second, TNA was applied to detect lipids in the liver of the water rat Nectomys squamipes. By using this natural model of hepatic steatosis (fat liver), a condition in which there is excessive accumulation of lipids, TNA provided a clearer identification of three species of polyunsaturated fatty acids (PUFAs) compared to other matrices. TNA presents better sensitivity and spectral resolution, little or no interference from matrix ions, high intensity of signal and low cost with high yield of matrix production.

Keywords: Lipid, MALDI-TOF, Nectomys squamipes, 9-aminoacridine.

1. Introduction

Matrix-assisted laser desorption/ionization time-of-flight mass spectrometry (MALDI-TOF MS) [1,2] has, as main characteristics, the easy sample production, soft ionization, easy operation, fast analysis and high accuracy. Mass spectrometry MALDI has been widely used in analyses of large molecules such as proteins [3], peptides [4], polysaccharides [5], oligonucleotides [6], Polymer [7,8], and DNA [9].

Despite MALDI MS being a powerful tool to analyze high mass molecules, its application to investigate small molecules is still a challenge due the fact that MALDI MS matrix cause interferences in the low molecular weight region (usually below *m/z* 500). An appropriate material to be used as matrix for MALDI MS analyses of small molecules must meet (*i*) strong absorption in the wavelength of the laser used, (*ii*) efficient ionization/desorption

*Corresponding author. E-mail: jeffersonsilvamartins@gmail.com

of the analytes, (*iii*) little or no fragmentation of the analyte and (*iv*) free of ions from the matrix that can interfere in the low *m/z* region [10–12]. Some of the new matrices for MALDI-TOF MS include graphene [13,14], carbon nanotubes [15], carbon dots [16], ionic liquids [17], metal-organic frameworks [18], molybdenum disulfide nanosheets/silver nanoparticles [19], among others.

In the last decades, the distribution of lipids in tissues and the structure and function of organelles rich in lipids have been investigated in mammal cells because of their association with many human diseases [20–24]. Mass spectrometry is one of the most important technologies applied in lipid analyses [25] and recent technical advances in MALDI mass spectrometry have allowed unprecedented knowledges about the role of lipids in neuronal functions [26], lipid imaging in mice brains [27] and lipid identification in the liver during hepatic steatosis [28], for example.

9-aminoacridine (9-AA) has been widely used as matrix in low mass regime analyses of lipids because its high sensibility and minimum background [8, 14, 27–33]. The 9-AA core structure also presents many applications in different areas. For instance, it can be used as specific marker [34], against neurodegenerative diseases and protozoa [35] and anticancer [36,37]. Many of these applications are directly related to the aromatic rings conjugation present in the 9-AA and its derivatives, resulting in a variety of energy absorption features in the electromagnetic spectrum.

In a previous work by some of us, Stroppa and coworkers [38,39] described a new compound named 2,4,5,7-tetranitro-9-aminoacridine (TNA) which was prepared from 9-aminoacridine hydrochloride monohydrate, nitric acid and sulfuric acid. Four nitro groups were introduced in the aromatic rings of 9-AA (position in the ring 2,4,5 and 7) using a nitration reaction (**Scheme 1**).

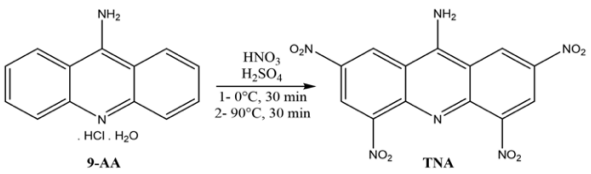

Scheme 1. Synthesis of TNA [38,39].

The emphasis of that work was the remarkable coloration change of the substance depending on the pH of the medium around the molecule, which makes it a candidate for novel pH indicators. Upon inspection of its UV-Vis spectra, presented in Figure 1, another interesting feature of TNA stood out: the new substance has a significantly bigger absorption in the wavelengths around 337 nm when compared with 9-AA, using the same molar concentration for both matrices. That is the wavelength of common lasers used in MALDI mass spectrometry, making TNA a candidate for a new matrix substance.

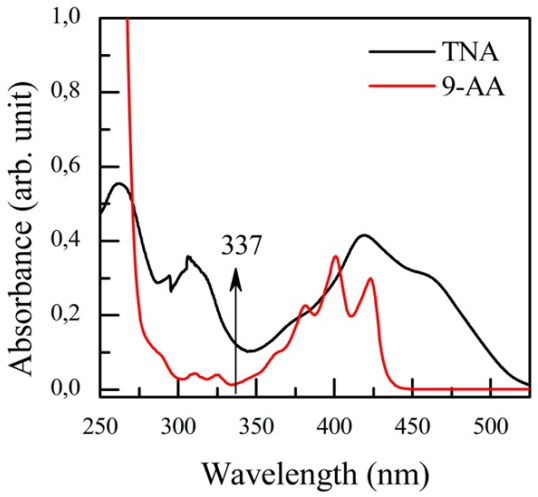

Figure 1. UV-VIS spectra obtained for TNA and 9-AA. Figure re-created from the data of [38,39].

In the present work, we investigated the use TNA, as a matrix for direct analysis of lipids in positive-ion mode by MALDI-TOF MS. First, we obtained direct Laser Desorption/Ionization mass spectra of TNA in order to identify characteristic peaks. Second, we compared the ion yield and spectral quality of MALDI spectra obtained for retinol using TNA, CHCA (alpha-cyano-4-hydroxycinnamic acid) and 9-AA as matrices. Remarkably, by applying TNA to a biological model of hepatic steatosis, a condition in which lipids are accumulated in the liver [28], we found that this matrix has a higher sensitivity and provides a clearer detection of lipids compared to normal 9-AA.

2. Material and Methods

2.1 Chemistry

9-aminoacridine hydrochloride monohydrate

98%, alpha-cyano-4-hydroxycinnamic acid (CHCA), and Retinol (Aldrich, São Paulo, Brazil), sulfuric acid 98% (Vetec, Rio de Janeiro, Brazil), nitric acid 65% (Cromoline, São Paulo, Brazil) methanol 99.8% (Alphatec, Paraná, Brazil), ethanol 99.8% (Neon Comercial, São Paulo, Brazil), acetoniteile 99.8% (Aldrich, São Paulo, Brazil). TNA was produced by our group for our previous work [38,39], a small 100 mL sample being extracted from stock.

2.2 Biological model and ethics statement

Adult specimens of *N. squamipes* were captured in the rural areas of the Municipality of Sumidouro (22° 02' 46" South and 42° 41' 21" West), located in the mountainous region of the state of Rio de Janeiro, Brazil, as before [28], and *Schistosoma mansoni*-infected *N. squamipes* were identified by the presence of adult worms in mesenteric veins using perfusion of the portal-hepatic system.

Animals were captured under authorization of Chico Mendes Institute for Biodiversity and Conservation of the Brazilian Government (ICMBIO, authorization number 13373). All procedures with *N. squamipes* were carried out in the field in accordance with biosafety standards level three. Biosafety techniques and personal safety equipment were used during all procedures according to the Brazilian Ministry of Health recommendations.

This study was carried out in full accordance with all international and Brazilian accepted ethic guidelines and was approved by the Oswaldo Cruz Foundation Ethics Committee on Animal Use ("CEUA-*Comissão de Ética no Uso de Animais"*, under protocol CEUA: LW81/12). CEUA follows the Brazilian national guidelines recommended by CONCEA ("*Conselho Nacional de Controle em Experimentação Animal"*).

2.3 Sample collection and histochemical detection of lipids

Liver fragments were fixed in a 4% paraformaldehyde solution overnight at 4°C, transferred to 0.1M phosphate buffer, pH 7.3, kept in 30% sucrose solution in phosphate buffer, pH 7.3, overnight at 4°C and frozen for further processing. Liver sections were then cut on a cryostat for both histological and MALDI-TOF analyses. The presence of lipids was confirmed in the liver cryo-sections by staining with Oil Red O (ORO) [1-(2,5-dimethyl-4-(2,5-dimethylphenyl) phenyldiazenyl azonapthalen-2-ol] (Sigma-Aldrich, USA), a lipid probe extensively used for histologic evaluation of hepatic steatosis [40–42] and other lipid disorders [43]. For quantitative evaluation of the lipid droplets (LDs) in the liver, ORO-stained sections were analyzed with a slide scanner (Pannoramic Histech 3D Scan, 3D Histech kft., Budapest, Hungary) and quantitative studies were performed using the *Pannoramic Viewer* and *Histoquant* softwares (3D Histech kft.) All staining and quantitative procedures were done as before [28].

2.4 Mass Spectrometry

All mass spectra were obtained using a Shimadzu Biotech Axima Performance apparatus, a Matrix Assisted Time of Flight Mass Spectrometer (MALDI-TOF) equipped with a Reflectron flight tube and a pulsed nitrogen laser, which operates at a wavelength of 337 nm. The apparatus is located at the "Laboratório de Colisões Atômicas e Superfícies, Departamento de Física, Federal University of Juiz de Fora, MG, Brazil". All Samples were deposited on wells of a stainless-steel multi-sample plate (model DE1580TA). Each spectrum consists of a sum of 200 profiles, generated by 40 laser shots each, at a rate of 20 shots per second. A raster method is used in which the laser shoots a slightly different position of the sample well for each profile. The Time of Flight of the instrument was operated in the Hi-Resolution, Reflectron mode, and the mass range used was m/z 100-1000. In the case of Retinol samples, preliminary experiments showed that a nominal laser power of 55 was enough to perform measurements with good mass resolution and acceptable signal-to-noise ratio. In the case of liver samples, a nominal laser power of 100 was required for all three matrices.

CHCA was used both as calibrant and as matrix. It was dissolved in a mixture of water of milli-Q quality and acetonitrile (1:1 v:v), containing also 0.1% TFA (trifloroacetic acid) in a concentration of about 5×10^{-2} mol/L. When used as calibrant, 0.7 µL of the solution was deposited alone on each of 6 wells, intercalated with other sample wells to reduce the calibration drift. Retinol was diluted in methanol, 10

mg/mL, as well as for the case of 9-AA. TNA was dissolved 1 mg/mL in acetonitrile.

In the case of Retinol, sample preparation followed the “dried droplet” method. Samples were spotted first and let dry. Matrices were spotted on top of the dried samples. To perform the analyses of the infected liver samples, 50 µm cryostat sections were placed on the bare sample wells, which subsequently were spotted with 1.0 µL of matrix solution and left to dry before inserting in the mass spectrometer.

3. Results

3.1 Laser desorption/ionization time of flight (LDI-TOF) of TNA

The LDI-TOF spectrometry experimentation shows that the TNA compound absorbs energy from the N_2 laser (λ = 337 nm) producing desorbed and ionized molecules without the need of a matrix, as can be seen at

Figure **2**. The LDI-TOF mass spectrum for TNA shows an ion peak $[M+H]^+$ *m/z* 375.0313 and other $[M+2H]^+$ (*m/z* 376.0437). It is also highlighted some possible fragments as $[M-NH_3]^+$ (*m/z* 358.3742) and $[M+Na]^+$ (396.9929). The theoretical value calculated for the TNA is $[M+H]^+$ *m/z* 375.0325.

3.2 Application of TNA to qualitative analysis of retinol

Next, to investigate the potential use of TNA in the detection of small lipids during MALDI-TOF MS routine applications, we performed a comparative study using retinol (commercial standard) as analyte. We compared TNA with the commercial matrices 9-AA and CHCA (Figure 3). The values found for ionized retinol ($[M]^+$) by TNA, 9-AA and CHCA were *m/z* 286.2278 (Figure 3a), *m/z* 286.2287 (Figure 3b) e *m/z* 286.2229 (Figure 3c), respectively.

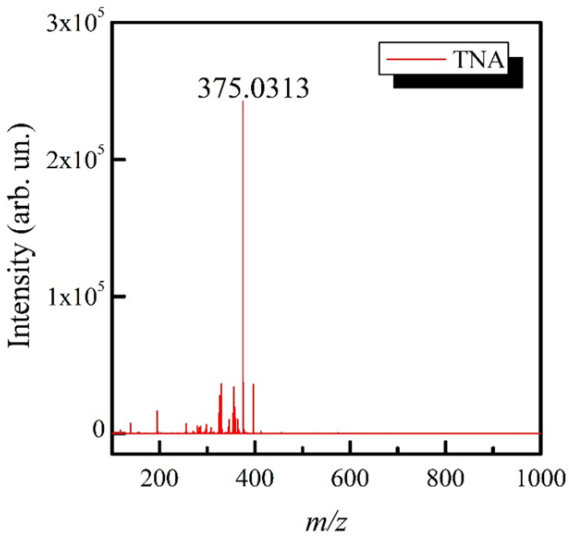

Figure 2. Ion intensity as a function of mass per charge for pure TNA sample diluted 1mg/mL in acetonitrile, without any other matrix. The most prominent peak at 375.013 is attributed to the protonated molecule.

In Figure 3(a), the mass spectrum of retinol obtained with TNA as matrix is much cleaner than the spectra obtained with the other matrices, shown in Figures 3(b) and 3(c). The intensity of matrix ions is almost negligible compared to the intensity of the retinol ion itself. This is in sharp contrast to both 9-AA and specially CHCA, wherein the matrix ions dominate the spectra. The absolute ion intensity of retinol is also an order of magnitude higher in the case of TNA than for the other matrices, thus resulting in a much-improved signal to noise ratio.

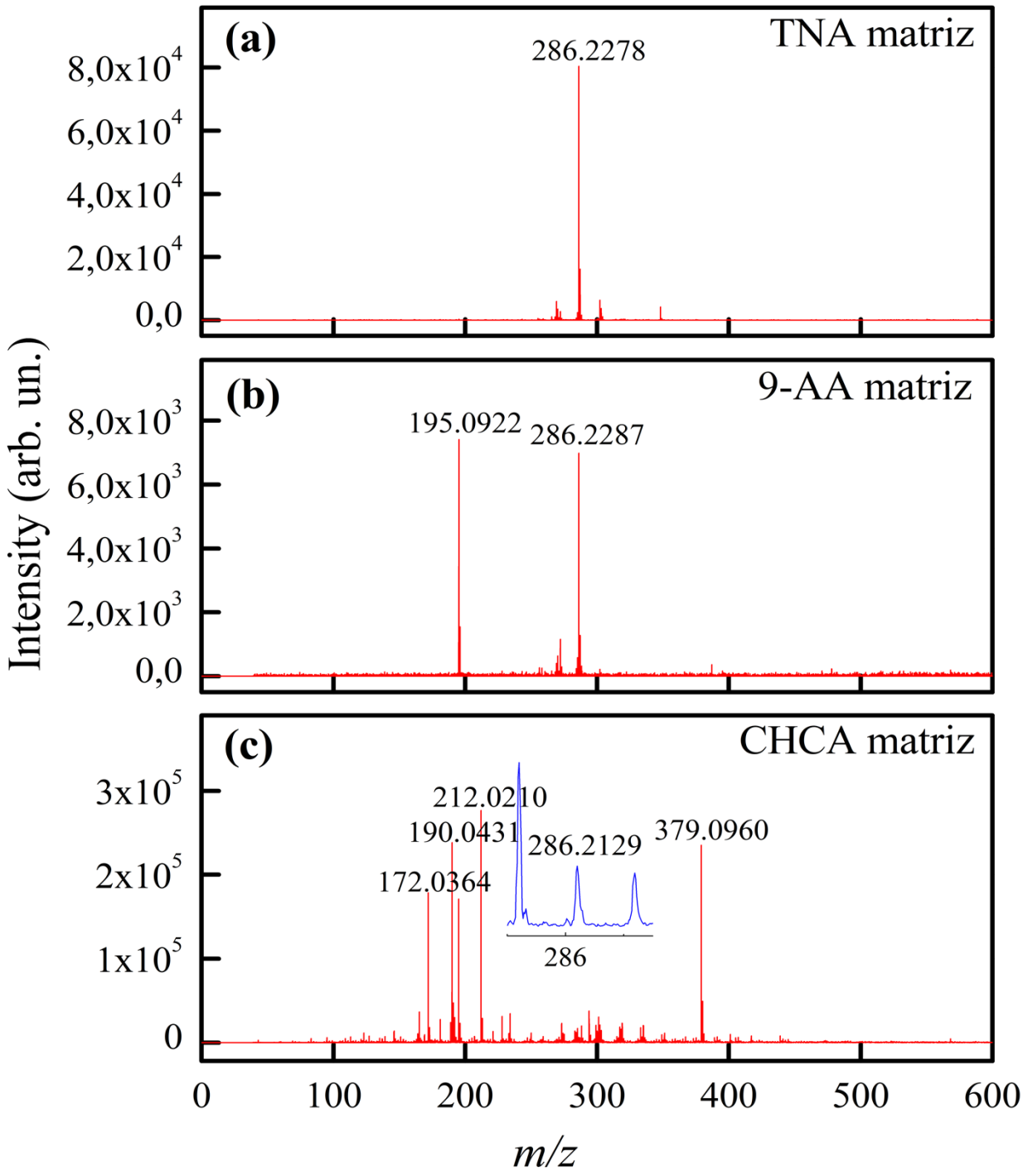

Figure 3: MALDI-TOF mass spectra of retinol obtained with (a) TNA, (b) 9-AA and (c) CHCA as matrices in the positive ion mode. Nominal laser power 55. The peaks at m/z 286.22 are attributed to ionized retinol molecule (M+) on all spectra. The other peaks are either contaminants or matrix fragments, especially in the case of panel (c). Note that in the case of TNA the parent matrix molecular ion is barely visible on this scale, providing a very clean background for the analyte.

3.2 Application of TNA for Identification of Lipid Ions by MALDI-TOF MS in biological specimens

To validate the use of TNA for lipid detection in biological samples, we next used a natural model of hepatic steatosis. The term hepatic steatosis refers to intracellular accumulation of lipids and subsequent formation of lipid droplets [44]. Steatosis of the liver may arise from a variety of situations and human diseases such as alcohol and metabolic syndrome, drugs or infectious diseases. Our group has recently demonstrated that hepatic steatosis occurs in response to the natural *Schistosoma mansoni* infection of the aquatic rat *Nectomys squamipes*, which is one of the main wild reservoir for this parasite in Brazil [28]. By using CHCA matrix, we previously demonstrated that three species of polyunsaturated fatty acids (PUFAs), the arachidonic acid (AA) $[M]^+$ (*m/z* 304.24), linoleic acid (LA) $[M+Na]^+$ (*m/z* 303.03) and oleic acid (OA) $[M+Na]^+$ (*m/z* 305.26) were consistently present in the hepatic tissue of infected *N. squamipes*. Therefore, we sought to identify the same lipids with TNA. Thus, new experiments were made with 9-AA and TNA matrices to detect the lipids AA, LA and OA in order to compare with the previous results obtained with the CHCA matrix.

Figure 3 shows MALDI-TOF mass spectra on the positive ion mode for samples of liver tissue of *N. squamipes* with the application of 9-AA and TNA matrices. In Figure 4a and 4b are presented mass spectra for a mass range from *m/z* 100 to 600 using the TNA and 9-AA matrices, respectively. By means of the results shown with the TNA matrix, we identified the peak *m/z* 303.1319 referring to LA $[M+Na]^+$, *m/z* 304.2419 indicative of AA $[M]^+$ and *m/z* 305.2574 referring to OA $[M+Na]^+$, as shown in **Erro! Fonte de referência não encontrada.**c. The appearance of protonated molecules $[M+H]^+$ and/or sodium adduct $[M+Na]^+$ are chemical events frequently observed during MALDI-TOF MS analyses on the positive ion mode [12,20,45,46]. The results with 9-AA matrix identified the peaks, *m/z* 303.1920, *m/z* 304.2455 e *m/z* 305.2992, referring to LA $[M+Na]^+$, AA $[M]^+$, OA $[M+Na]^+$, respectively (Figure d).

The discussed results showed that the application of TNA matrix was capable to ionize and detect the analytes present in the fat liver because the values found were strongly correlated with the theoretical values of the lipids analyzed. Moreover, the mass spectrum obtained for the hepatic tissue showed additional advantages when we used the TNA matrix (Figure a), since a baseline with a low signal/noise ratio and with a strong signal intensity was detected. The high presence of lipids in the liver was confirmed by *in situ* direct detection of lipids by histological analyses after ORO staining (Fig. 4ef). Histoquantitative analyses revealed the occurrence of 3.89 ± 0.49 lipid droplets per 100 μm^2 of hepatic tissue.

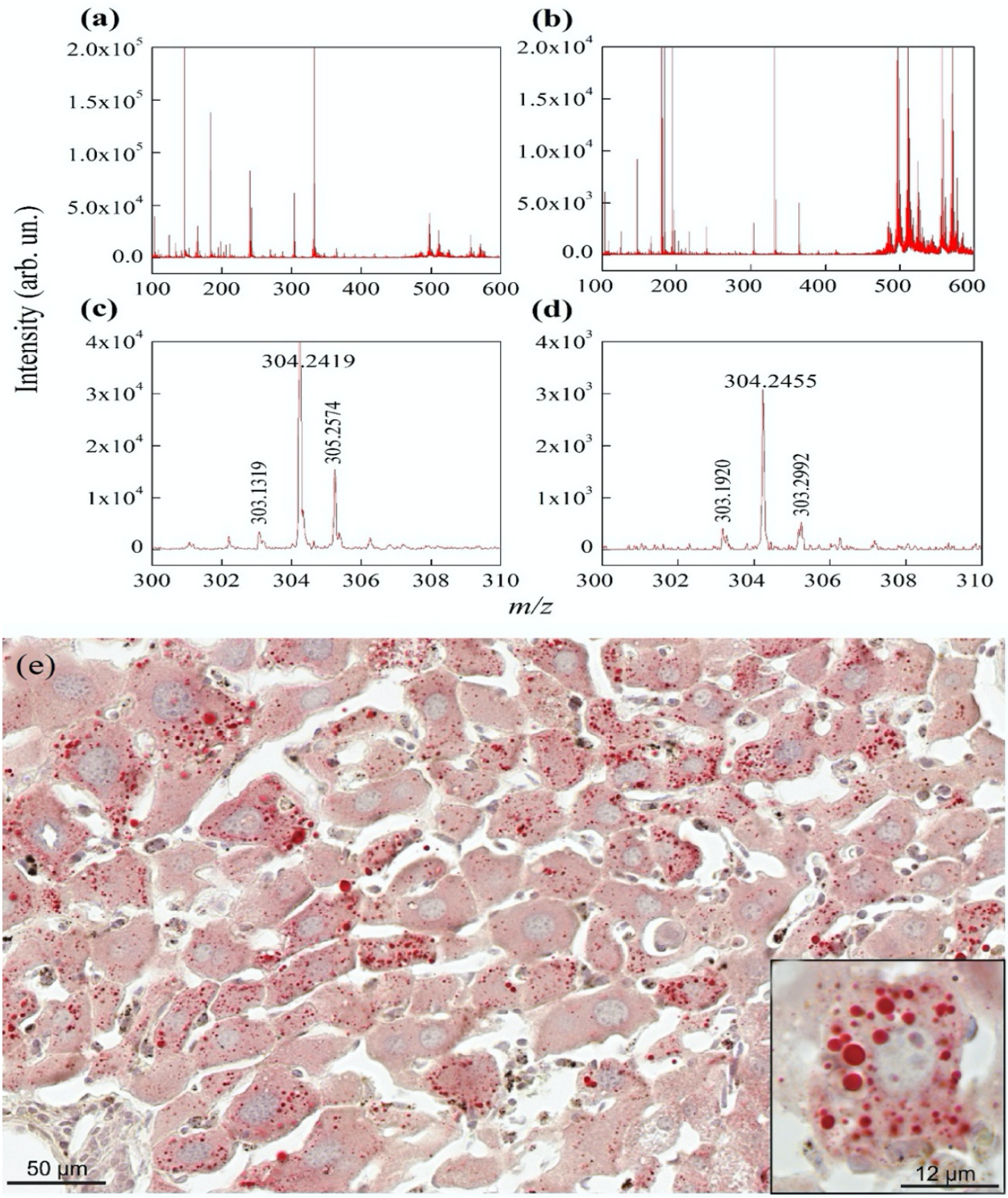

Figure 4. Liver sections from animals with natural hepatic steatosis analyzed with MALDI-TOF mass spectra (a-d) and after staining with Oil Red O (ORO), a specific lipid probe (e-f). Note in (e), the presence of numerous lipid droplets seen as round organelles (stained in red) and distributed within hepatocytes. In (f), a hepatocyte is seen in high magnification. Nominal laser power was 100. MALDI-TOF and histological analyses were performed on cryosections. Detection and quantification of lipid droplets per area of hepatic tissue were done after ORO staining in a slide scanner using the *Pannoramic Viewer* and *Histoquant* softwares (3D Histech kft.).

4. Conclusions

This work demonstrates that TNA is a useful matrix for analysis of lipids by MALDI-TOF MS. The TNA matrix allowed detection of intact retinol ions with less fragmentation (i.e. softer ionization process). Later, this new matrix was applied to fat liver for the identification of the lipids OA, LA and AA. The TNA matrix showed many advantages when compared with the commercial matrix such as better quality and spectral resolution in terms of sensibility, few or none interference from matrix ions, high intensity of the signal detected and low cost with high output during matrix preparation. We conclude that the new TNA matrix for MALDI MS is a promising material to be used in the identification of lipids in biological systems.

Acknowledgments

The authors thank CNPq, CAPES, FAPEMIG and FINEP, for financial support.

5. References

[1] Karas, M.; Bachmann, D.; Bahr, U.; Hillenkamp, F. *Int. J. Mass Spectrom. Ion Process.* 1987, *78*, 53–68. https://doi.org/10.1016/0168-1176(87)87041-6.

[2] Karas, M.; Hillenkamp, F. *Anal. Chem.* 1988, *60* (20), 2299–2301. https://doi.org/10.1021/ac00171a028.

[3] Calvano, C. D.; Picca, R. A.; Bonerba, E.; Tantillo, G.; Cioffi, N.; Palmisano, F. *J. Mass Spectrom.* 2016, *51* (9), 828–840. https://doi.org/10.1002/jms.3823.

[4] Novotná, K.; Šedo, O.; Havel, J. In *Collection Symposium Series*; Institute of Organic Chemistry and Biochemistry, Academy of Sciences of the Czech Republic: Prague, 2003; Vol. 6, pp 65–68. https://doi.org/10.1135/css200306065.

[5] López-García, M.; García, M. S. D.; Vilariño, J. M. L.; Rodríguez, M. V. G. *Food Chem.* 2016, *199*, 597–604. https://doi.org/10.1016/j.foodchem.2015.12.016.

[6] Costanzo, G.; Pino, S.; Timperio, A. M.; Šponer, J. E.; Šponer, J.; Nováková, O.; Šedo, O.; Zdráhal, Z.; Di Mauro, E. *PLoS One* 2016, *11* (11), e0165723. https://doi.org/10.1371/journal.pone.0165723.

[7] Martins, J. S.; Borges, B. G. A. L.; Machado, R. C.; Carpanez, A. G.; Grazul, R. M.; Zappa, F.; Melo, W. S.; Rocco, M. L. M.; Pinho, R. R.; Lima, C. R. A. *Eur. Polym. J.* 2014, *59*, 1–7. https://doi.org/10.1016/j.eurpolymj.2014.07.005.

[8] Lima, C. R. A.; Martins, J. S.; Pinheiro, C.; Avila, L. F.; Pinho, R. R.; Rocco, M. L. M.; Melo, W. S.; Zappa, F. *J. Polym. Sci. Part B Polym. Phys.* 2019, *57* (15), 967–972. https://doi.org/10.1002/polb.24851.

[9] Eszlinger, M.; Müller, S.; Bösenberg, E.; Moll, A.; Paschke, R. *Can. J. Diabetes* 2016, *40* (5), S4. https://doi.org/10.1016/j.jcjd.2016.08.011.

[10] Chen, R.; Chen, S.; Xiong, C.; Ding, X.; Wu, C.-C.; Chang, H.-C.; Xiong, S.; Nie, Z. *J. Am. Soc. Mass Spectrom.* 2012, *23* (9), 1454–1460. https://doi.org/10.1007/s13361-012-0421-z.

[11] Hillenkamp, F.; Peter-Katalinić, J. *MALDI MS: A Practical Guide to Instrumentation, Methods and Applications*; 2007.

[12] Hoffmann, E. de.; Stroobant, V. *Mass Spectrometry : Principles and Applications*; J. Wiley, 2007.

[13] Wei, H.; Wei, J.; Zhang, Z.; Wang, Y.; Zhang, J. *RSC Adv.* 2016, *6* (72), 67833–67838. https://doi.org/10.1039/C6RA10447A.

[14] Sun, J.; Chen, S.; Liu, H.; Xiong, C.; Wang, J.; Xie, X.; Xue, J.; Chen, P.; Nie, Z. *RSC Adv.* 2016, *6* (102), 99714–99719. https://doi.org/10.1039/C6RA21083J.

[15] Pan, C.; Xu, S.; Hu, L.; Su, X.; Ou, J.; Zou, H.; Guo, Z.; Zhang, Y.; Guo, B. *J. Am. Soc. Mass Spectrom.* 2005, *16* (6), 883–892. https://doi.org/10.1016/j.jasms.2005.03.009.

[16] Chen, Y.; Gao, D.; Bai, H.; Liu, H.; Lin, S.; Jiang, Y. *J. Am. Soc. Mass Spectrom.* 2016, *27* (7), 1227–1235. https://doi.org/10.1007/s13361-016-1396-y.

[17] Li, Y. L.; Gross, M. L. *J. Am. Soc. Mass Spectrom.* 2004, *15* (12), 1833–1837. https://doi.org/10.1016/j.jasms.2004.08.011.

[18] Wang, S.; Niu, H.; Zeng, T.; Zhang, X.; Cao, D.; Cai, Y. *Microporous Mesoporous Mater.* 2017, *239*, 390–395. https://doi.org/10.1016/j.micromeso.2016.10.032.

[19] Zhao, Y.; Deng, G.; Liu, X.; Sun, L.; Li, H.; Cheng, Q.; Xi, K.; Xu, D. *Anal. Chim. Acta* 2016, *937*, 87–95. https://doi.org/10.1016/j.aca.2016.06.026.

[20] Toledo, D. A. M.; Roque, N. R.; Teixeira, L.; Milán-Garcés, E. A.; Carneiro, A. B.; Almeida, M. R.; Andrade, G. F. S.; Martins, J. S.; Pinho, R. R.; Freire-de-Lima, C. G.; Bozza, P. T.; D'Avila, H.; Melo, R. C. N. *PLoS One* 2016, *11* (8), 1–22. https://doi.org/10.1371/journal.pone.0160433.

[21] Murphy, D. J. *Protoplasma* 2012, *249* (3), 541–585. https://doi.org/10.1007/s00709-011-0329-7.

[22] Beller, M.; Thiel, K.; Thul, P. J.; Jäckle, H. *FEBS Lett.* 2010, *584* (11), 2176–2182. https://doi.org/10.1016/j.febslet.2010.03.022.

[23] Fujimoto, T.; Ohsaki, Y.; Cheng, J.; Suzuki, M.; Shinohara, Y. *Histochem. Cell Biol.* 2008, *130* (2), 263–279. https://doi.org/10.1007/s00418-008-0449-0.

[24] Melo, R. C. N.; Weller, P. F. *J. Leukoc. Biol.* 2014, *96* (5), 703–712. https://doi.org/10.1189/jlb.3RU0214-110R.

[25] Li, L.; Han, J.; Wang, Z.; Liu, J.; Wei, J.; Xiong, S.; Zhao, Z. *Int. J. Mol. Sci.* 2014, *15* (6), 10492–10507. https://doi.org/10.3390/ijms150610492.

[26] Gross, R. W.; Jenkins, C. M.; Yang, J.; Mancuso, D. J.; Han, X. *Prostaglandins Other Lipid Mediat.* 2005, *77* (1-4 SPEC. ISS.), 52–64. https://doi.org/10.1016/j.prostaglandins.2004.09.005.

[27] Wang, X.; Han, J.; Chou, A.; Yang, J.; Pan, J.; Borchers, C. H. *Anal. Chem.* 2013, *85* (15), 7566–7573. https://doi.org/10.1021/ac401595a.

[28] Amaral, K. B.; Silva, T. P.; Malta, K. K.; Carmo, L. A. S.; Dias, F. F.; Almeida, M. R.; Andrade, G. F. S.; Martins, J. S.; Pinho, R. R.; Costa-Neto, S. F.; Gentile, R.; Melo, R. C. N. *PLoS One* 2016, *11* (11), e0166979. https://doi.org/10.1371/journal.pone.0166979.

[29] Liu, H.; Chen, R.; Wang, J.; Chen, S.; Xiong, C.; Wang, J.; Hou, J.; He, Q.; Zhang, N.; Nie, Z.; Mao, L. *Anal. Chem.* 2014, *86* (20), 10114–10121. https://doi.org/10.1021/ac5034566.

[30] Vaidyanathan, S.; Goodacre, R. *Rapid Commun. Mass Spectrom.* 2007, *21* (13), 2072–2078. https://doi.org/10.1002/rcm.3063.

[31] Jana Becher, Alexander Muck, Axel Mithöfer, A. S. and W. B. *Rapid Commun. mass Spectrom.* 2008, *22*, 1153–1158. https://doi.org/10.1002/rcm.

[32] Vermillion-Salsbury, R. L.; Hercules, D. M. *Rapid Commun. Mass Spectrom.* 2002, *16* (16), 1575–1581. https://doi.org/10.1002/rcm.750.

[33] Soltzberg, L. J.; Hagar, A.; Kridaratikorn, S.; Mattson, A.; Newman, R. *J. Am. Soc. Mass Spectrom.* 2007, *18* (11), 2001–2006. https://doi.org/10.1016/j.jasms.2007.08.008.

[34] Jesionowski, T.; Przybylska, A.; Kurc, B.; Ciesielczyk, F. *Dye. Pigment.* 2011, *88* (1), 116–124. https://doi.org/10.1016/j.dyepig.2010.05.011.

[35] Sebestik, J.; Hlavacek, J.; Stibor, I. *Curr Protein Pept Sci* 2007, *8* (5), 471–483. https://doi.org/10.2174/138920307782411400.

[36] Narayanan, R.; Tiwari, P.; Inoa, D.; Ashok, B. T. *Life Sci.* 2005, *77* (18), 2312–2323. https://doi.org/10.1016/j.lfs.2005.03.020.

[37] Malachowska-Ugarte, M.; Cholewinski, G.; Dzierzbicka, K.; Trzonkowski, P. *Eur. J. Med. Chem.* 2012, *54*, 197–201. https://doi.org/10.1016/j.ejmech.2012.04.040.

[38] Stroppa, P. H. F.; Martins, J. da S.; Quirino, W. G.; da Silva, A. D. INPI, n. BR 10 2016 026223-2, Brazil, 2016, 2016.

[39] Stroppa, P. H. F.; Glanzmann, N.; Duarte, L. M.; Sato, R. T.; De Oliveira, M. A. L.; Da Silva, A. D. *Artic. J. Braz. Chem. Soc* 2017, *00* (00), 1–7. https://doi.org/10.21577/0103-5053.20170084.

[40] Ge, F.; Lobdell, H.; Zhou, S.; Hu, C.; Berk, P. D. *Exp. Biol. Med.* 2010, *235* (11), 1282–1286. https://doi.org/10.1258/ebm.2010.010095.

[41] Levene, A. P.; Kudo, H.; Armstrong, M. J.; Thursz, M. R.; Gedroyc, W. M.; Anstee, Q. M.; Goldin, R. D. *Histopathology* 2012, *60* (6), 971–981. https://doi.org/10.1111/j.1365-2559.2012.04193.x.

[42] Demir, Ş.; Ünübol, M.; Aypak, S. Ü.; İpek, E.; Aktaş, S.; Ekren, G. S.; Yılmaz, M.; Tunca, R.; Güney, E. *Int. J. Endocrinol.* 2016, *2016*, 1–7. https://doi.org/10.1155/2016/5083746.

[43] Melo, R. C. N.; D'Avila, H.; Wan, H.-C.; Bozza, P. T.; Dvorak, A. M.; Weller, P. F. *J. Histochem. Cytochem.* 2011, *59* (5), 540–556. https://doi.org/10.1369/0022155411404073.

[44] Anderson, N.; Borlak, J. *Pharmacol. Rev.*

2008, *60* (3), 311–357. https://doi.org/10.1124/pr.108.00001.

[45] Allison, P.-C. L. and J. 1995, *30* (November 1994), 408–423.

[46] Fuchs, B.; Süß, R.; Schiller, J. *Prog. Lipid Res.* 2010, *49*, 450–475. https://doi.org/10.1016/j.plipres.2010.07.001.